Front. Chem. China 2010, 5(2): 150–161
DOI 10.1007/s11458-010-0113-9

FEATURE ARTICLE

Structure-property relationships of organic dyes with D-π-A structure in dye-sensitized solar cells

Zhong-Sheng WANG (✉)[1] and Fang LIU[1,2]

1 Laboratory of Advanced Materials, Department of Chemistry, Fudan University, Shanghai 200438, China
2 College of Chemistry and Chemical Engineering, Inner Mongolia University, Hohhot 010021, China

Organic dyes with a D-π-A structure have drawn increasing attention as sensitizers in dye-sensitized solar cells (DSSCs), due to their rich photophysical properties, easy molecular tailoring, and low-cost production. This review mainly focuses on the relationship between dye structure and photovoltaic properties for organic dyes containing cyanoacrylic acid as both an anchor and an acceptor. This review also introduces different donors and π-conjugation units as building blocks for sensitizer synthesis.

Keywords D-π-A structure, dye-sensitized solar cells

1 Introduction

The production of greenhouse gases from our ever increasing consumption of fossil fuels is aggravating the problem of global warming and threatening the quality of life here on Earth. In addition, increasing global demands for energy and limited petroleum and coal reserves will restrict future economic development. It is thus necessary and important to exploit renewable energy sources, such as solar energy, to maintain sustainable social and economic development.

Although photovoltaics have been dominated by devices based on crystalline or amorphous silicon-based solar cells, recent attention has been paid to mesoscopic inorganic and organic semiconductors, commonly referred to as "bulk" junctions because of their interconnected three-dimensional structure. The possible advantages of bulk-junction devices include very low fabrication costs and good compatibility with flexible substrates. The most advanced of these new devices is the dye-sensitized solar cell (DSSC).

The working principle of a DSSC is shown in Figure 1. Light absorption in the DSSC is executed by dye molecules attached to a wide band gap nanostructured semiconducting material, such as titania, followed by electron injection from excited dye molecules to the conduction band of the semiconductor. The resultant oxidized dye molecule is reduced to its original state by I^- ions in the electrolyte.

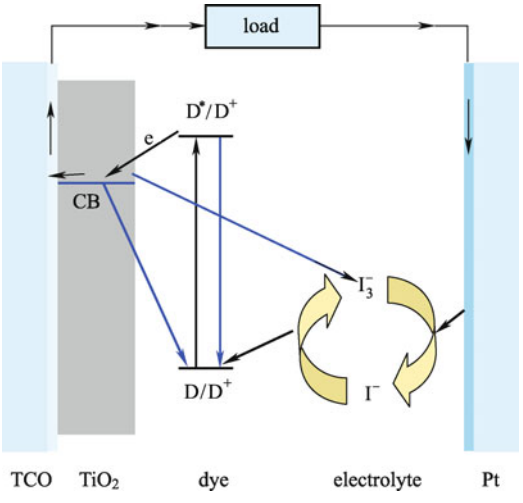

Figure 1 Working principle of a DSSC.

Concomitantly I^- is oxidized to its oxidized form, I_3^-, and the latter is later reduced back to I^- by accepting electrons at the counter electrode. The electric circuit is completed by diffusion of I^- and I_3^- from and to the counter electrode, respectively. The difference between the Fermi energy level of titania under light and the redox potential of the redox couple I_3^-/I^- is in principle the open-circuit photovoltage (V_{oc}).

A progress milestone was made with DSSCs in 1991 when O'Regan and Grätzel reported that they had achieved an overall solar-to-electric power conversion efficiency (η) of 7.9% [1]. In 1993, an η of 10% was achieved using cis-di

Received December 31, 2009; accepted March 5, 2010
E-mail: zs.wang@fudan.edu.cn

(thiocyanato)bis(2,2'-bipyridyl-4,4'-dicarboxylate)ruthenium (II), namely N3 (Figure 2), as the sensitizer [2]. For the first time, a molecular photovoltaic device had reached the efficiency of traditional Si-based solar cells. In 2001 they synthesized a panchromatic dye, $\{(C_4H_9)_4N\}_3[Ru(Htcterpy)(NCS)_3]$ (tcterpy = 4,4′,4″-tricarboxy-2,2′:6′,2″-terpyridine), the so-called black dye (Figure 2), giving over 80% incident photon-to-electron conversion efficiency (IPCE) in a broad wavelength range from 400 to 700 nm and achieving very efficient sensitization over the whole visible range extending into the near-IR region up to 920 nm [3]. A DSSC based on the so-called black dye produced a short-circuit photocurrent density (J_{sc}) of 20.5 mA·cm^{-2} and an η of 10.4%, which was certified by a photovoltaic calibration laboratory (NREL, USA). The photovoltaic performance of the black dye superseded that of the N3 sensitizer due to its superior panchromatic light harvesting properties combined with nearly quantitative electron injection yield from the excited dye into the conduction band of the nanocrystalline TiO_2 film.

Many efforts have been made to optimize the performance of DSSCs toward higher efficiency using the above-mentioned outstanding dyes: N3 (or N719) and black dye [4–10]. To date, a few groups have achieved an η of greater than 10% in the laboratory [8–13]. An η of 11.1% obtained by Han and coworkers is the highest certified η of DSSC so far [12]. In principle, an ideal DSSC should produce a J_{sc} of about 23 mA·cm^{-2}, a V_{oc} of about 0.85 V and fill factor (FF) of about 0.75, corresponding to an η of about 15% [14]. Therefore, to improve η to its maximum value is still a big challenge. One of the main factors limiting device performance is low J_{sc} because the reported dye sensitizers cannot harvest photons from solar emissions completely, especially in the spectral region above 700 nm. For this reason, molecular design and synthesis of new efficient dyes is of the utmost significance [15–20].

Considering the high cost of ruthenium and the synthetic complexity of ruthenium-based dyes, scientists have turned their interests to metal-free organic dyes. Metal-free organic dyes have three major advantages over ruthenium-based dyes. One is that organic dyes have high molar extinction coefficients than those of metal complexes due to their much higher oscillator strengths. The use of organic dyes would allow a thinner TiO_2 film to harvest the incident light efficiently. Secondly no noble metal such as ruthenium is concerned in organic dyes. This reduces the overall cost of device production. The third advantage is the potential for facial molecular design and structural tailoring. For these reasons, organic dyes may find future application in DSSCs. In general, the molecular structure of an organic dye for DSSC use has been designed and synthesized based on several basic concepts: 1) matching of the oxidation potentials of the ground and exited states for a dye, which are usually represented by the highest occupied molecular orbital (HOMO) and the lowest unoccupied molecular orbital (LUMO), with the energy levels of the I^-/I_3^- redox potential and the conduction band energy level of the TiO_2 electrode, respectively; 2) a donor–π-conjugation-linkage–acceptor (D-π-A) structure required for a wide range absorption extending into the near-infrared or infrared regions; 3) one or two anchoring groups such as a carboxylic acid or sulfonic acid group required for a strong adsorption onto the surface of the TiO_2.

Based on the given general synthetic concepts for organic dyes, hundreds of organic dyes have been prepared for use in DSSCs. Direct comparisons of reported dyes in terms of performance parameters favor further optimization of dye structure for high efficiency. Since the efficiencies reported from different groups and sometimes from different researchers in the same group are not comparable, it is sometimes misleading to compare solar cell performance for different dyes directly. To obtain reliable performance information, one should keep in mind the following three points: 1) use of an AM1.5G solar simulator, whose emission spectrum is well matched with that of a standard AM1.5G solar emission spectrum; 2) calibration of the light intensity with a crystalline Si solar cell, which has already been calibrated in a national photovoltaic calibration laboratory; 3) use of a mask, whose aperture area should be greater than or equal to 95% but smaller than 100% of that for the dye-loaded TiO_2 film, covering all the exposed surface of the DSSC surrounding the active layer to avoid diffuse light due to light refraction and reflection of the exposed glass around the dye-loaded TiO_2

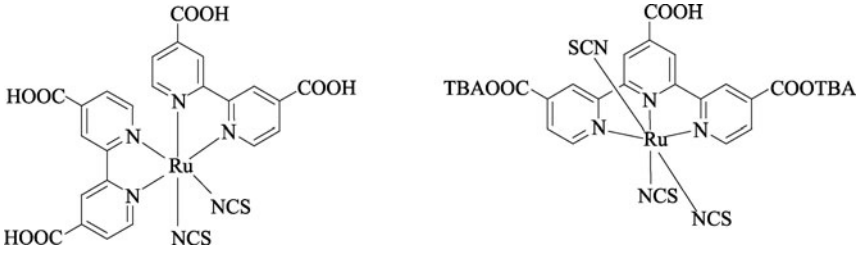

Figure 2 Structures of N3 and the black dye.

film. The aperture area of the mask should be measured correctly with a precise method of measurement. The efficiency of DSSCs cannot be measured correctly without observing the above-mentioned three points. For example, the light intensity coming from an AM1.5 solar simulator was determined to be 113 $mW \cdot cm^{-2}$, but only gave a reading of 67 $mW \cdot cm^{-2}$ on a power or radio meter. It is evident that J_{sc} and η can be overestimated by about 70% if the light intensity of white light is calibrated by a power or radio meter rather than a standard calibration Si solar cell.

For the metal-free organic dyes reported in DSSCs, the number of dyes having a cyanoacrylic acid subunit as both acceptor and anchor outnumbers those having other kind of acceptors. According to the reported results, a lot of dyes with a cyanoacrylic acid subunit produce an η of greater than 7%, only a few dyes with other acceptors such as rhodanine-3-acetic acid achieve an η of above 7%. This review introduces dyes with cyanoacrylic acid as the acceptor and mainly discusses the effect of the donor and π-conjugation unit on absorption properties and photovoltaic performance; structure-photovoltaic-property relationships of congener dyes are also discussed. In this review, metal-free organic dyes will be grouped based on different π-conjugation systems, and in each section dyes with various donors will be presented.

2 Dyes with a methine chain

Organic dyes were already used as sensitizers in DSSCs before 2000, but efficiency at that stage was low [21–23]. Significant progress on metal-free organic dye based DSSCs was made by Arakawa's group and Huang's group, when they reported that cyanine [24] and hemicyanine [25,26] dyes were promising for use in DSSCs. Thereafter increasing efforts have been devoted to the design and synthesis of metal-free organic dyes with a D-π-A structure as sensitizers of TiO_2 in DSSCs.

Cyanoacrylic acid as an acceptor and anchor in an organic dye sensitizer was first reported by Hara et al. [27]. Dyes **3**, **4** and **5** (Figure 3) were synthesized by respectively inserting 1, 2, and 3 methine units between a coumarin derivative and cyano-carboxyl group [27,28]. It was found that the maximum absorption gradually redshifted when increasing the number of methine units from 1 to 3. Although dye **5**, with three methine units, showed the broadest feature of photocurrent action spectrum among the series of dyes, the IPCE value at the maximum absorption was much lower than those of the other two dyes, mainly due to dye aggregation. Strong interactions between dye molecules of **5** on the TiO_2 surface resulted in H-aggregation and diminished both J_{sc} and V_{oc} [29]. Among the three coumarin-methine dyes, dye **4** with two methine units showed the highest J_{sc} of 14.0 $mA \cdot cm^{-2}$ and highest η of 6.0%.

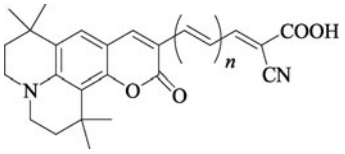

Figure 3 Structures of dyes **3** (n = 0), **4** (n = 1), and **5** (n = 2).

Replacement of the coumarin moiety in dyes **3**, **4** and **5** with N,N-dimethylaminophenyl (DMA) forms dyes **6**, **7** and **8** (Figure 4), which have been studied by two Japanese groups [30–32]. The replacement of the donor leads to significant hypsochromic shift of the maximum absorption peak, indicating that the coumarin derivative is a stronger donor than the DMA group. As a result, dye **7** produces a lower J_{sc} and η than dye **4** (Table 1). To redshift the maximum absorption peak, two DMA groups, the donors, were linked to a π-conjugation system containing three methine units, and dye **9** (Figure 5) was obtained [30,31]. Hara et al. found that two donors are better than one donor to improve the values of J_{sc} and η. Table 1 shows comparative data on photovoltaic performance for dyes with one and two donors. Dye **8** with one donor, synthesized by Yanagida and coworkers [32] produced an η of 3.6% (J_{sc} = 10.4 $mA \cdot cm^{-2}$, V_{oc} = 0.62 V, FF = 0.56). The η was significantly improved to 6.8% (J_{sc} = 12.9 $mA \cdot cm^{-2}$, V_{oc} = 0.71 V, FF = 0.74) when two donors were employed [31]. When the methyl group was replaced with an ethyl group on the donor part of dye **9**, dye **10** was prepared and a similar efficiency was obtained [32]. Also included in Table 1 is a comparison between dye **4** and dye **7**. Since the coumarin derivative donates electrons more strongly than DMA, the maximum absorption peak is redshifted from dye **7** to dye **4**. Due to an extended absorption spectrum, dye **4** produced a much higher J_{sc} than dye **7**.

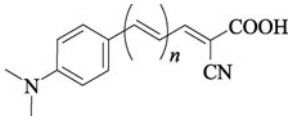

Figure 4 Structures of dyes **6** (n = 0), **7** (n = 1) and **8** (n = 2).

Table 1 Comparison of properties for dyes **8** with **9** and **7** with **4**

Dye	J_{sc} /($mA \cdot cm^{-2}$)	V_{oc} / V	FF	η/%	Ref.
8	10.4	0.62	0.56	3.6	[32]
9	12.9	0.71	0.74	6.8	[30, 31]
7	9.9	0.74	0.74	5.4	[30, 31]
4	14.0	0.60	0.71	6.0	[28]

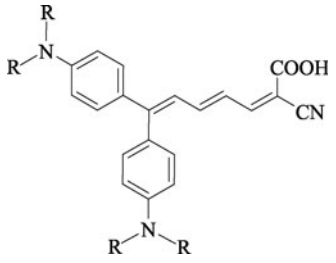

Figure 5 Structures of dyes **9** (R = methyl) and **10** (R = ethyl).

Replacement of DMA with a triphenylamine (TPA) unit in dye **7**, forming dye **11** (Figure 6), induced redshift of the maximum absorption due to an increase in the electron donating ability of the phenylamino moiety. Comparison of absorption properties for dyes **4**, **7**, and **11** shows that the donating ability increases from DMA, through TPA, to the coumarin derivative. Redshift of the maximum absorption can also be realized by expanding the π-conjugation of the donor moiety via linking a vinyl unit to one phenyl ring of the TPA unit in dye **11** [33]. J_{sc} and η were thus improved significantly from dye **11** to dye **12** (Figure 6) as stated by Chen and coworkers [33].

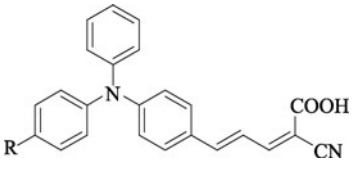

Figure 6 Structures of dyes **11** (R = H) and **12** (R = vinyl).

Phenothiazine is also a promising donor for application in DSSCs. Sun and coworkers developed dye **13** (Figure 7) by simply bridging one carbon-carbon double bond between phenothiazine and cyanoacrylic acid [34]. This dye showed a maximum absorption peak at 452 nm in CH_2Cl_2 but blue shifted to 425 nm upon adsorption on TiO_2 [34]. The authors mentioned that dye **13** was simple in structure and easy to synthesize. This dye produced an η of 5.5% (J_{sc} = 10.9 mA·cm^{-2}, V_{oc} = 0.712 V, FF = 0.71).

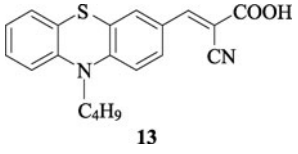

13

Figure 7 Structure of dye **13**.

3 Dyes with a thiophene chain

Although extension of π-conjugation by increasing the number of methine units redshifts absorption to longer wavelength region, it simultaneously causes two problems: first, it complicates the synthetic procedure, and second, it increases the instability of the dye molecule, owing to potential fission of carbon-carbon double bonds and structural isomerization.

In 2003, Arakawa and coworkers proposed introducing aromatic ring moieties, such as thiophene, between the donor and acceptor [35]. Dyes **14**–**16** (Figure 8) were synthesized by respectively inserting one, two and three thiophene moieties between a coumarin derivative and a cyanoacrylic acid moiety [35,36]. The number of thiophene units did not significantly affect the UV-Vis absorption peak position both in solution (500–510 nm) and on TiO_2 (around 460 nm), but the absorption threshold increased with increasing number of thiophene units. Dye adsorption usually decreases with increasing the molecular size. In contrast, adsorption increased when increasing the number of thiophene units. This was because adding more thiophene unit led to stronger π-π stacking, and gave greater dye adsorption. Interestingly, dye **16** produced a lower maximum IPCE than the other two dyes. Electrochemical analysis revealed that dye **16** has a lower LUMO than dyes **14** and **15**, leading to insufficient driving force for electron injection. This phenomenon suggests that the LUMO energy level tends to decrease with increasing number of thiophene units due to enlarged π-conjugation arising from increased π-π stacking. Dye **16** produced a lower IPCE than the other two dyes due to its lower LUMO, which led to lower values of J_{sc} and η. Among the three dyes, dye **15** produced an η of 7.4% with a mask under AM 1.5G irradiation (100 mW·cm^{-2}) with J_{sc} of 13.5 mA·cm^{-2}, V_{oc} of 0.71 V, and FF of 0.77.

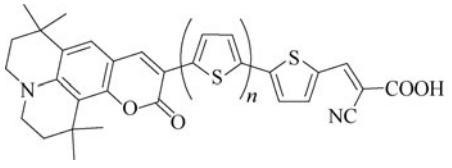

Figure 8 Structures of dyes **14** (n = 0), **15** (n = 1), and **16** (n = 2).

Following the report by Hara et al., several donors were used to replace the coumarin derivative, hoping to achieve broader absorption and hence higher efficiency. However, no breakthrough has been achieved in terms of both absorption and efficiency among the dyes with a thiophene π-conjugation system.

Replacement of the donor part in dye **14** with TPA formed dye **17** (Figure 9), which showed an absorption maximum at 404 nm both in acetonitrile and on TiO_2 [37]. Due to very narrow range absorption properties, dye **17** only produced an η of 2.75% with J_{sc} of 5.42 mA·cm^{-2}, V_{oc} of 735 mV, and FF of 0.69 [37]. This dye was also tested by another group, but

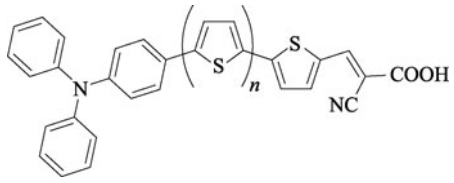

Figure 9 Structures of dyes **17** (n = 0), **18** (n = 1), and **19** (n = 2).

the value of η increased dramatically to 5.20% due to a very high J_{sc} of 12.8 mA·cm^{-2} obtained by the authors, which seems to be an overestimated judgement from the narrow absorption and IPCE action spectra [38]. Expansion of π-conjugation by insertion of 2 and 3 thiophene units between TPA and the acceptor formed dyes **18** and **19** [39], as shown in Figure 9. Dyes **17**, **18**, and **19** respectively showed blue shift of the absorption maximum, as compared to dyes **14**, **15**, and **16**. This indicates that TPA is a weaker donor than the coumarin derivative. It is reasonable, therefore, that dyes **17**, **18**, and **19** produced lower J_{sc} values than dyes **14**, **15**, and **16**, respectively, under the same conditions. When hexyloxy groups were installed in the para-positions of the two benzene rings of TPA, a light-resistant dye **20** (Figure 10) was prepared and the maximum absorption peak redshifted by 20 nm in ethanol [40,41], due to destabilization of the HOMO caused by the hexyloxy groups. Strikingly, the IPCE was still close to 90% at 600 nm where the light absorption of the sensitizer in solution was very small. This important redshift in the photocurrent response can be attributed to lateral interactions in the adsorbed monolayer of the sensitizer. Under standard global AM1.5 solar conditions, the dye-**20**-sensitized cell gave a J_{sc} value of 14.10 mA·cm^{-2}, V_{oc} of 728 mV and FF of 0.71, which corresponded to an η of 7.25%. A solar cell employing the light-resistant dye with spiro-OMeTAD as a hole-transporting material exhibited a J_{sc} of 9.64 mA·cm^{-2}, V_{oc} of 798 mV, and FF of 0.57, corresponding to an η of 4.4% in standard AM 1.5 sunlight.

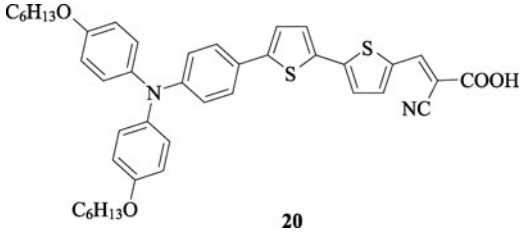

20

Figure 10 Structure of dye **20**.

Asymmetric organic dyes **21** and **22** (Figure 11) were prepared by using the bulky difluorenylphenylamine (DFPA) as the donor [42]. They showed maximum absorptions at 436 and 452 nm in ethanol for dyes **21** and **22**, respectively. Dye

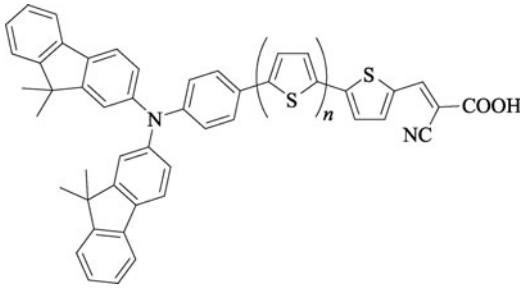

Figure 11 Structures of dyes **21** (n = 0) and **22** (n = 1).

22 produced an η of 8.0% with a J_{sc} of 14.0 mA·cm^{-2}, V_{oc} of 0.753 V, and FF of 0.76. Dye **15** and dye **22** are similar in structure except for the donor moiety, their comparative data are shown in Table 2. Dye **22** generated a higher V_{oc} than dye **15**, probably due to its higher LUMO and less aggregation. Although the reported J_{sc} of dye **22** is higher than that of dye **15**, this may result from different solar irradiation because dye **15** should generate a higher J_{sc} than dye **22** according to absorption and IPCE spectra.

An indolo[1,2-f]phenanthridine unit was chosen as the electron donating unit to synthesize dyes **23** and **24** (Figure 12) by Ko and coworkers [43]. Dye **23** displayed absorption bands at 339 and 453 nm, while dye **24** showed an intense and broad absorption band at 410 nm in THF. It was thought that the two thiophene moieties in dye **24** seemed to contribute to broadening of the absorption peak. Although dye **24** exhibited an absorption maximum at 410 nm, it produced an η of 8.34% with a J_{sc} of 15.81 mA·cm^{-2}, V_{oc} of 0.73 V and FF of 0.72.

The efficiency dropped significantly when julolidine was used as the donor. Dye **25** (Figure 13) comprising bithiophene showed two absorption bands at 352 and 462 nm in ethanol. Although dye **25** showed redshift of absorption peaks as compared to dye **24**, the former dye only produced an η of 2.47% with a J_{sc} of 6.26 mA·cm^{-2}, V_{oc} of 0.61 V and FF of 0.64 [44]. They observed that the twisted geometry of the dye led to blue shift of the maximum absorption. The twisted non-planar geometry thus affected the solar cell performance.

Dyes **26**, **27**, and **28** (Figure 14) with rigid structure were synthesized by Sun and coworkers using a tetrahydroquinoline derivative as the donor [45]. Among the three dyes, dye **27** produced the highest η of 4.53%. They suggest that a rigid molecular structure as well as a suitable larger π-conjugation system is helpful for creating dyes with higher η in DSSCs.

4 Dyes with other π-conjugation units

It is known that thiophene moieties are good π-conjugation units for constructing efficient organic dye sensitizers. To

Table 2 Comparison of dyes **15** and **22**

Dye	λ_{max}/nm	IPCE onset/nm	J_{sc}/(mA·cm^{-2})	V_{oc}/V	FF	η/%	Ref.
15	511	820	13.5	0.71	0.77	7.4	[36]
22	452	720	14.0	0.753	0.76	8.0	[42]

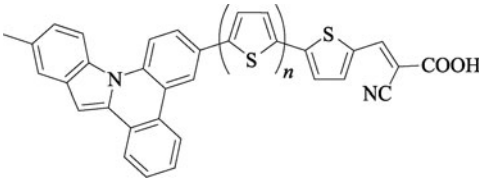

Figure 12 Structures of dyes **23** (n = 0) and **24** (n = 1).

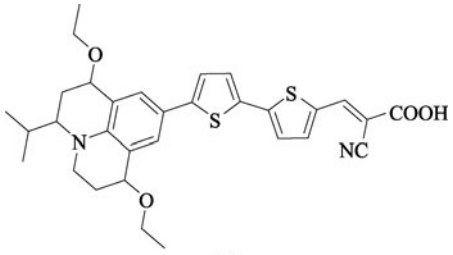

Figure 13 Structure of dye **25**.

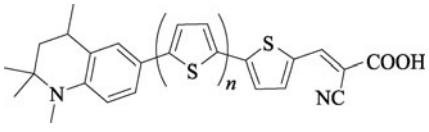

Figure 14 Structures of dyes **26** (n = 0), **27** (n = 1), and **28** (n = 2).

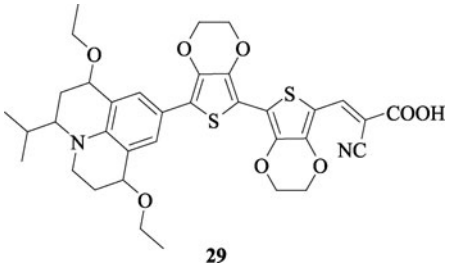

Figure 15 Structure of dye **29**.

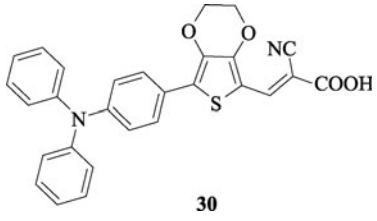

Figure 16 Structure of dye **30**.

optimize the structures of metal-free organic dyes, several functionalizations of the thiophene bridge were approached. For example, an electron donating group such as an ethylenedioxy group, was introduced into the 3,4-position of the thiophene unit. Ko and coworkers reported dye **29** (Figure 15) containing 3,4-ethylenedioxythiophene (EDOT) as a spacer [44]. Replacing the two thiophene units in dye **25** with two EDOT units resulted in a bathochromic shift of 44 nm and a 1.41 × 10^4 L·mol^{-1}·cm^{-1} increase of the absorption coefficient (ε) in the absorption spectrum due to a more delocalized π-conjugated system. However, dye **29** with julolidine as the donor part exhibited an extremely low η of 0.74% owing to its stronger aggregation on the TiO_2 electrode.

Chou and coworkers developed a quite simple dye, dye **30** (Figure 16), bearing one EDOT unit as the linker [38]. The introduction of the EDOT group between the TPA and cyanoacrylic acid increased the spectral response as compared with dye **17**. This perhaps rendered a better degree of charge separation, resulting in a leap in the photovoltaic performance in comparison to dye **17**. The onset of the IPCE spectrum was at about 660 nm, and high IPCE performance ($>$ 80%) was observed from 400 to 570 nm, with the highest value, 92%, at 450 nm. Under the standard AM1.5G irradiation, the η for the dye-**30**-sensitized solar cell with an active cell area of 0.25 cm^2 was calculated to be 7.3%, with a J_{sc} of 15.5 mA·cm^{-2} and a V_{oc} of 690 mV, while dye **17** produced an η of 5.2% under the same conditions.

The combination of DFPA with EDOT formed dyes **31** and **32** (Figure 17), prepared by Wang and coworkers [46]. The photovoltaic parameters (J_{sc}, V_{oc}, FF, and η) of dye **32** were 15.68 mA·cm^{-2}, 746 mV, 0.711, and 8.32%, respectively. By employing a similar titania film and electrolyte, they obtained an η of 7% using the DSSC with the counterpart dye **22** with a bithiophene unit. They attributed the improved efficiency with dye **32** to its better spectral match with the solar irradiance due to introduction of the biEDOT unit.

Wang and coworkers developed dye **33** (Figure 18), which consisted of thienothiophene unit as a spacer and DFPA as the electron donor. An η of 7% along with excellent stability was provided by a DSSC based on dye **33** when using a solvent-free ionic liquid electrolyte [47]. Furthermore, for the first time, an η of 4.8% was reached for an all-solid-state DSSC

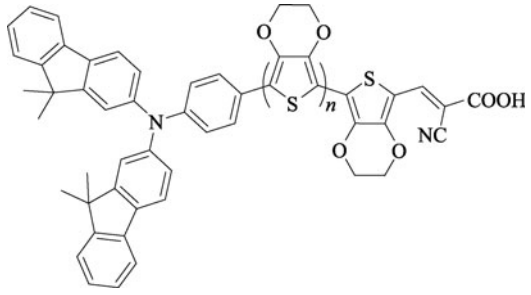

Figure 17 Structures of dyes **31** (n = 0) and **32** (n = 1).

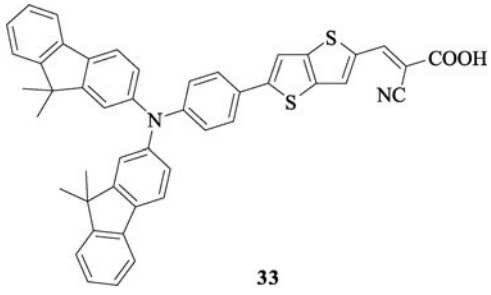

33

Figure 18 Structure of dye **33**.

based on a metal-free organic dye, even though its spectral response did not match well with the AM1.5G solar emission. They also obtained organic dye **34** containing thienothiophene as a spacer but TPA as the donor, and found that a strong electron donor can raise the HOMO considerably but the LUMO only slightly [48]. Dye **34** (Figure 19) also showed an η of about 7% with a solvent-free ionic liquid electrolyte. Insertion of a second thienothiophene unit into the conjugated bridge (dye **35**, Figure 19) resulted in a bathochromic shift of 8 nm along with an increase of the absorption coefficient (ε) by $5 \times 10^3\ \mathrm{L \cdot mol^{-1} \cdot cm^{-1}}$ [49]. A sensitizer **35** based DSSC demonstrated an η of 8% using a volatile liquid electrolyte and an η of 6.5% with a solvent-free ionic liquid electrolyte under AM1.5G sunlight [49].

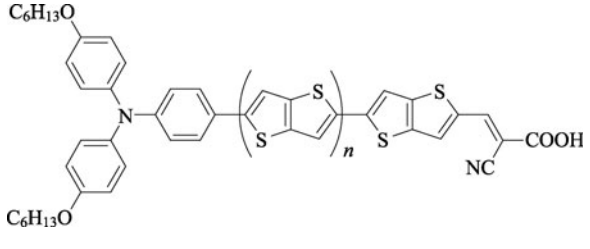

Figure 19 Structures of dyes **34** (n = 0) and **35** (n = 1).

In addition to thienothiophene, dithienothiophene was also used as a spacer in DSSCs and it was first reported by Sun and coworkers [50]. Replacing the thiophene unit with a dithienothiophene unit, a weak bathochromic shift of 3 nm along with an intense increase of the absorption coefficient (ε) by $10^4\ \mathrm{L \cdot mol^{-1} \cdot cm^{-1}}$ could be observed in the absorption spectrum. With tetrahydroquinoline as the electron donor, an η of 2.34% was achieved for DSSCs based on dye **36** [50], whose structure is shown in Figure 20.

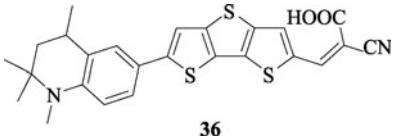

36

Figure 20 Structure of dye **36**.

Wang and coworkers developed dye **37** (Figure 21) containing dithienothiophene as a spacer and DFPA as a donor [51]. It showed a high ε of $4.48 \times 10^4\ \mathrm{L \cdot mol^{-1} \cdot cm^{-1}}$ at 525 nm due to intramolecular charge transfer transition. The DSSC based on dye **37** showed an η of 8.0% under an irradiance of AM 1.5G. Moreover, in combination with a solvent-free ionic liquid electrolyte, an η of 7% was demonstrated, with an excellent stability measured under dual thermal and light soaking stress.

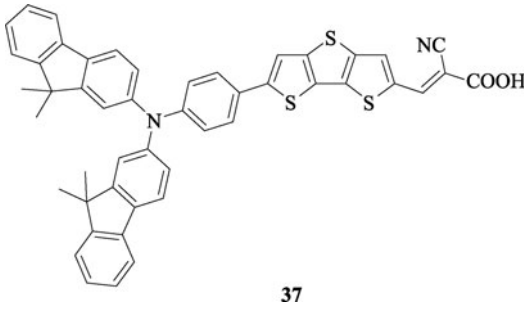

37

Figure 21 Structure of dye **37**.

Müllen and coworkers developed a series of bulky ladder-type pentaphenylene-based dyes (Figure 22) with the same acceptor (cyanoacrylic acid) and different donors (diphenylamino **38**, phenothiazinyl **39**, and bis(N,N-4-dimethylaminophenyl)amino **40**) [52]. A large spacer can facilitate effective charge separation and induce a high ε value of around $7.0 \times 10^4\ \mathrm{L \cdot mol^{-1} \cdot cm^{-1}}$. However a long spacer can also weaken donor-acceptor interactions and therefore induce the main absorption band to exist around 450 nm. η's of 2.3%, 1.8%, and 1.1%, respectively, were achieved with DSSCs based on dyes **38**–**40**.

5 Dyes with different conjugation units

Jiang et. al. synthesized dye **41** (Figure 23) with an EDOT unit as a spacer to bridge between di-*p*-tolylaminophenyl and

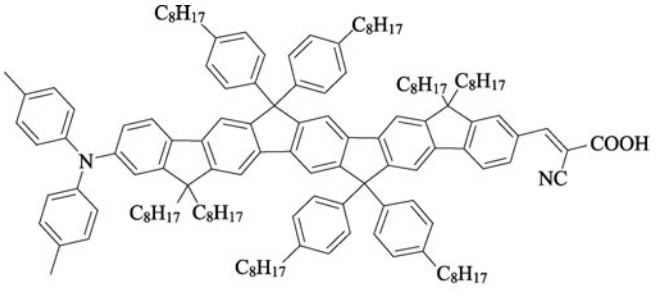

38

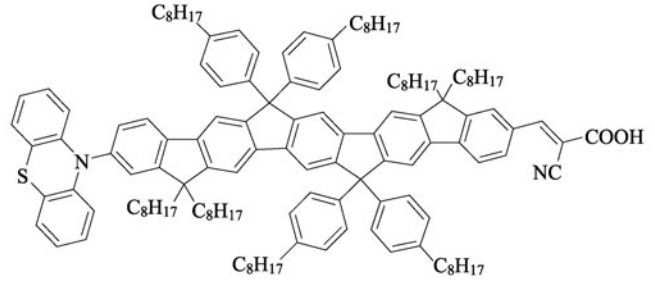

39

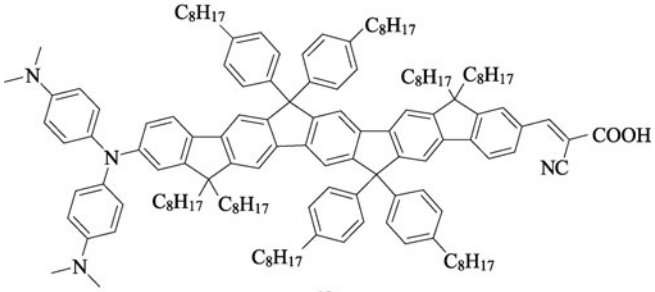

40

Figure 22 Structures of dyes **38**, **39**, and **40**.

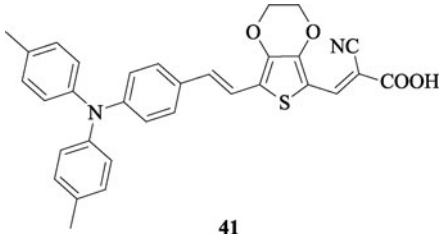

41

Figure 23 Structure of dye **41**.

cyanoacrylic acid. The absorption maximum was located at 460 nm with a high ε of 4.67×10^4 L·mol^{-1}·cm^{-1} [53]. Under AM1.5 sunlight irradiation, the DSSC employing dye **41** as the sensitizer demonstrated an η value of 7.33%. Yang and coworkers expanded π-conjugation of dye **41** by introducing more conjugation units such as thiophene, EDOT, and carbon-carbon double bonds. DSSCs based on the obtained dyes **42** (Figure 24) and **43** (Figure 25) produced η values of 6.03% and 3.59%, respectively [54].

Dye **44** (Figure 26) was prepared by Hara and coworkers by

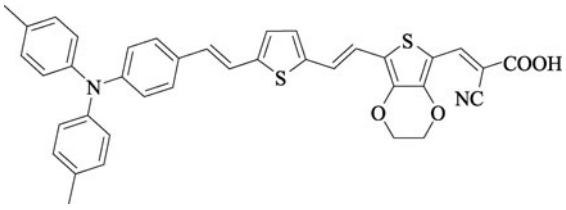

Figure 24 Structure of dye **42**.

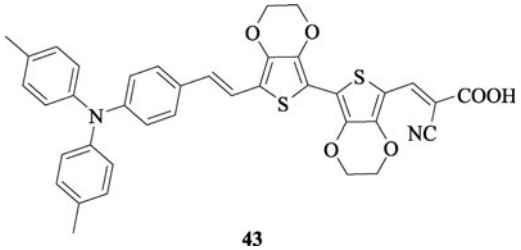

43

Figure 25 Structure of dye **43**.

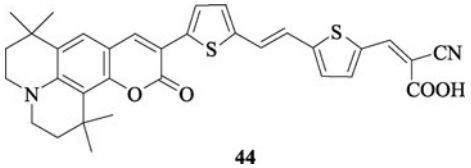

44

Figure 26 Structure of dye **44**.

inserting one carbon-carbon double bond between the two thiophene moieties in dye **15**. This structural modification redshifted the maximum absorption by 15 nm, and therefore enhanced J_{sc} by about 18% [55]. The value of η improved from 7.1% (J_{sc} = 13.5 mA·cm^{-2}, V_{oc} = 0.69 V, FF = 0.76) for dye **15** to 8.2% (J_{sc} = 15.9 mA·cm^{-2}, V_{oc} = 0.69, FF = 0.75) for dye **44** under the same conditions [55]. Introduction of a cyanovinylene group to the bithiophene in dye **15** formed dye **45** (Figure 27), which absorbed more intensively at longer wavelength (λ = 552 nm, ε = 97400 L·mol^{-1}·cm^{-1}) than the counterpart dye **15** (λ = 511 nm, ε = 64300 L·mol^{-1}·cm^{-1}) [56]. Dye **45** exhibited a light harvesting efficiency of near unity, in 6 μm thick transparent TiO_2 films, and an IPCE greater than 80% in the range 430–660 nm, with photo-response onset at 850 nm. As a result, under illumination by AM1.5G simulated solar light (100 mW·cm^{-2}), dye **45** generated J_{sc} values as high as 18.8 mA·cm^{-2} in such thin TiO_2 films. Compared with the dyes containing one –CN group, dye **45** having two –CN groups in the π-conjugation bridge positively shifts the LUMO and thus redshifting the maximum absorption band [57].

Wang and coworkers have investigated organic dye **46** (Figure 28) which features triarylamine as the electron-donating moiety and cyanoacrylic acid as electron-accepting

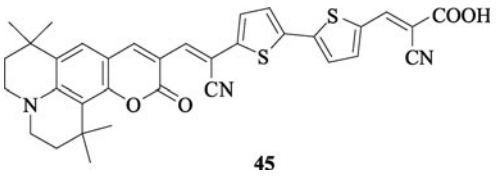

45

Figure 27 Structure of dye **45**.

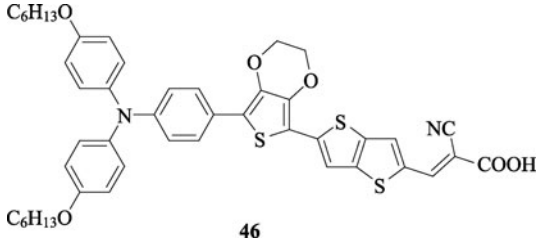

46

Figure 28 Structure of dye **46**.

moiety linked by an EDOT-thienothiophene bridge [58]. The UV-Vis absorption spectrum of dye **46** had one intense visible absorption band centered at 552 nm, which suggests that dye **46** is a wide spectral response organic chromophore for DSSCs. In conjunction with a volatile acetonitrile electrolyte and a solvent-free ionic liquid electrolyte, η values of 9.8% and 8.1% measured under AM1.5G full sunlight have been reached for DSSCs.

6 Dye aggregation

For planar organic dyes, dye aggregation or π-π stacking becomes a more serious problem when increasing the conjugated system chain. Thus solar cell performance (IPCE, J_{sc}, V_{oc}) diminishes due to strong intermolecular π-π interactions. To reduce such interactions, and hence dye aggregation, additives such as deoxycholic acid (DCA) were used to co-graft with the dye molecules. For example, co-adsorption of DCA with dye **44** not only improved J_{sc} but also enhanced V_{oc} [55]. When 120 mmol·L^{-1} DCA was dissolved in a solution of dye **44**, η was improved from 5.0% (J_{sc} = 12.0 mA·cm^{-2}, V_{oc} = 0.59 V, FF = 0.71) to 8.2% (J_{sc} = 15.9 mA·cm^{-2}, V_{oc} = 0.69 V, FF = 0.75). The enhanced J_{sc} was attributed to the improved electron injection yield because isolated dye molecules are more efficient than dye aggregates for electron injection. The increased V_{oc} resulted from retarded charge recombination, revealed by the increased electron lifetime with increasing co-adsorbed amount of DCA [55].

Although co-adsorption can improve solar cell performance significantly, it simultaneously decreases dye adsorption remarkably, which thus decreases light harvesting efficiency. It is therefore wise to reduce intermolecular interactions or dye aggregation by means of molecular design. By introducing a side ring to the alkene chain in dye **5**, dye **47** (Figure 29) was obtained [59]. Dye **5** exhibited a maximum absorption at 513 nm, while dye **47** had a maximum absorption band at 492 nm in ethanol. Upon adsorption onto TiO_2, 50 nm and 5 nm blue shifts were observed for dyes **5** and **47**, respectively. The side ring linked to the alkene chain was found to be effective at preventing dye aggregation. For this reason, DCA was not needed as a co-adsorbent with dye **47** on the TiO_2 surface, ensuring a high surface concentration of the dye and efficient photon-to-electron conversion. From dye **5** to **47**, the extra side ring resulted in remarkable improvement in J_{sc} and V_{oc}. The IPCE action spectrum of dye **47** was broad with a maximum IPCE value of 84% and onset at 800 nm. Dye **47** produced an η of 6.7% under illumination by simulated solar light (100 mW·cm^{-2}) with a J_{sc} of 16.1 mA·cm^{-2}, V_{oc} of 0.60 V and FF of 0.69.

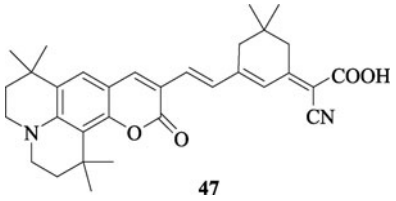

47

Figure 29 Structure of dye **47**.

Tian and coworkers prepared dye **48** (Figure 30) with the same side ring as in dye **47** [60]. This dye had a maximum absorption band at 497 nm in acetonitrile and exhibited IPCE greater than 80% in the spectral range 430–630 nm with photoelectric response onset at 760 nm [60]. It was found that there was no significant π-aggregation with dye **48** on the surface of TiO_2 film due to the twisted structure arising from the indoline unit and isophorone segment. This dye produced an η of 7.41% (AM 1.5, 100 mW·cm^{-2}) with a J_{sc} of 18.63 mA·cm^{-2}, V_{oc} of 634 mV and FF of 0.63.

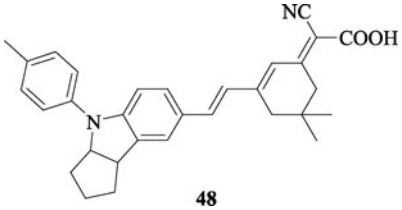

48

Figure 30 Structure of dye **48**.

Tian and coworkers reported dyes with D-D-π-A configuration [61]. Introduction of a starburst TPA group as the electron-donor unit brought about improved photovoltaic performance as compared with the single TPA unit counterpart. It may be a promising way to inhibit aggregation

between molecules and enhance the stability of the solar cells. By adding additional donor moieties to the outside of the donor group, the HOMO and LUMO energy levels can be conveniently tuned. The DSSCs based on dye **49** (Figure 31) showed a maximum IPCE of 85%, J_{sc} of 13.8 mA·cm^{-2}, V_{oc} of 0.63 V, and FF of 0.69, corresponding to an η of 6.02% under AM1.5G simulated solar irradiation (100 mW·cm^{-2}).

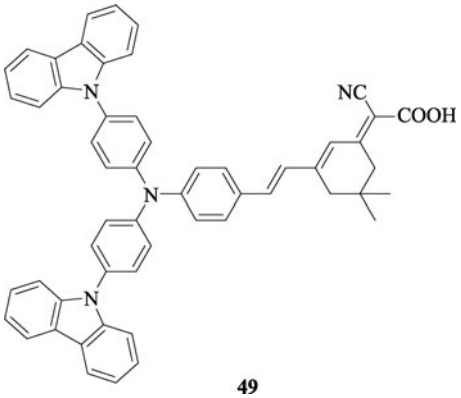

49

Figure 31 Structure of dye **49**.

Organic dyes which have a carbazole derivative as an electron donor and a cyanoacrylic acid moiety as an electron acceptor and anchoring group, connected with n-hexyl-substituted oligothiophenes as a π-conjugated system, were designed and synthesized for prevention of dye aggregation [62]. As compared to dye **50** (Figure 32), the presence of an alkyl chain in dye **51** (Figure 33) retarded charge recombination and increased electron lifetime by about 9 times [63]. Simultaneously, 80 mV of V_{oc} enhancement was observed from dye **50** to **51** [63]. The V_{oc} enhancement was attributed to the hydrophobic alkyl chains, which block I_3^- ions approaching the TiO_2 surface, and prevent close π-π stacking of dye molecules as well. An η of 7.6% was obtained for dye **52** (Figure 33) with the typical electrolyte containing 0.05 mol·dm^{-3} I_2, and was improved to 8.3% (J_{sc} = 15.22 mA·cm^{-2}, V_{oc} = 0.73 V, and FF = 0.75) under 100 mW·cm^{-2} simulated AM1.5G solar irradiation by increasing the iodine concentration to 0.2 mol·dm^{-3}. This improvement was due to enhanced diffusion of I_3^- ions.

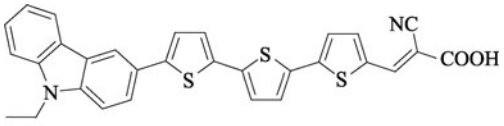

50

Figure 32 Structure of dye **50**.

DSSCs comprising dye **52** as the sensitizer and an ionic liquid (IL) as the electrolyte produced an η of 7.6% [64],

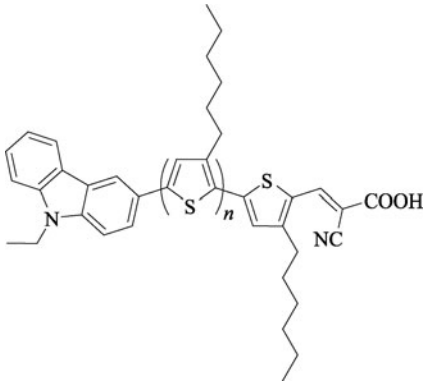

Figure 33 Structures of dyes **51** (n = 2) and **52** (n = 3).

which was comparable to that with a volatile organic liquid electrolyte. This makes an interesting contrast to the case of DSSCs employing the conventional Ru complex sensitizer (N719), whose efficiency decreased dramatically when the volatile electrolyte was replaced with an IL. As a result, with the IL electrolyte, the value of η with dye **52** was higher than that with N719. The result was mainly attributed to longer electron lifetime in the DSSCs with dye **52**. The longer electron lifetime is remarkable because with conventional volatile electrolytes, the electron lifetimes with many organic dyes including dye **52** were shorter than that with N719. This high compatibility of dye **52** with an IL electrolyte shows that molecular modification of organic dyes can overcome the disadvantages for both ILs and organic dyes, mostly originating from their high viscosities and from short electron lifetime observed with volatile electrolytes, respectively. Long-term stability of DSSCs with dye **52** and an IL electrolyte was also investigated, showing an η greater than 7% for 2000 h under continuous illumination of one sun.

7 Conclusions

Organic dyes have been extensively investigated for application in DSSCs, and a lot of organic dyes with a D-π-A structure, including many other dyes [65–71] that are not present in this review, have been developed by means of wise molecular design and synthesis. Great success has been achieved, with efficiency improving smoothly over the past 10 years. However, the efficient dye sensitizers reported so far usually have absorption bands below 550 nm, indicating that photons in the longer wavelength region are not utilized efficiently. For those dyes whose maximum absorption is above 550 nm, they are able to harvest incident light in a wide spectral range, but the obtained photocurrent and efficiency are not as high as expected due to their insufficiently high LUMOs. From the point of view of matching energy levels, efficient panchromatic organic dyes should be designed by

fine tuning of the HOMO and LUMO through wise combinations of the electron donor, π-conjugation unit, and electron acceptor with assistance from molecular tailoring. The fast progress of metal-free organic dye based DSSCs, which have potential high efficiency, good long-term stability, and low cost, foretells of good prospects for their application in DSSC technology. This review, in combination with other reviews on organic dye sensitized solar cells published recently [72,73], is anticipated to provide instructions to further push the development of DSSCs.

Acknowledgements The work was supported by the National Natural Science Foundation of China (Grant Nos. 20971025 and 90922004), the Shanghai Pujiang Program (Grant No. 09PJ1401300), the Shanghai Innovation Program of Science and Technology (Grant No.10530705300), Shanghai Leading Academic Discipline Project (B108), and the Scientific Research Foundation for the Returned Overseas Chinese Scholars, State Education Ministry.

Zhong-Sheng WANG obtained his doctoral degree in science from Peking University in the Prof. Chun-Hui Huang's group, where he completed his doctoral dissertation on dye-sensitized solar cells. After conducting research and development of dye-sensitized solar cells in NIMS and AIST, Japan for 7 years, he joined the Institute of New Energy, Fudan University as a full professor in 2008. His research interests include donor-π-conjugation-acceptor and metal-complex dyes, wide-band-gap semiconducting nanomaterials, quantum dots, and ionic liquids for application in sensitized solar cells.

References

1. O'Regan, B.; Grätzel, M., *Nature* **1991**, *353*, 737–740
2. Nazeeruddin, M. K.; Kay, A.; Rodicio, I.; Humphry-Baker, R.; Mueller, E.; Liska, P.; Vlachopoulos, N.; Graetzel, M., *J. Am. Chem. Soc*. **1993**, *115*, 6382–6390
3. Péchy, P.; Renouard, T.; Zakeeruddin, S. M.; Humphry-Baker, R.; Comte, P.; Liska, P.; Cevey, L.; Costa, E.; et al., *J. Am. Chem. Soc*. **2001**, *123*, 1613–1624
4. Zaban, A.; Chen, S. G.; Chappel, S.; Gregg, B. A., *Chem. Commun*. **2000**, 2231–2232
5. Jung, H. S.; Lee, J. K.; Nastasi, M.; Lee, S. W.; Kim, J. Y.; Park, J. S.; Hong, K. S.; Shin, H., *Langmuir* **2005**, *21*, 10332–10335
6. Tennakone, K.; Kumara, G. R. R. A.; Kottegoda, I. R. M.; Perera, V. P. S., *Chem. Commun*. **1999**, 15–16
7. Wang, Z. S.; Huang, C. H.; Huang, Y. Y.; Hou, Y. J.; Xie, P. H.; Zhang, B. W.; Cheng, H. M., *Chem. Mater*. **2001**, *13*, 678–682
8. Wang, Z. S.; Kawauchi, H.; Kashima, T.; Arakawa, H., *Coord. Chem. Rev*. **2004**, *248*, 1381–1389
9. Wang, Z. S.; Yanagida, M.; Sayama, K.; Sugihara, H., *Chem. Mater*. **2006**, *18*, 2912–2916
10. Wang, Z. S.; Yamaguchi, T.; Sugihara, H.; Arakawa, H., *Langmuir* **2005**, *21*, 4272–4276
11. Nazeeruddin, M. K.; De Angelis, F.; Fantacci, S.; Selloni, A.; Viscardi, G.; Liska, P.; Ito, S.; Takeru, B.; et al., *J. Am. Chem. Soc*. **2005**, *127*, 16835–16847
12. Chiba, Y.; Islam, A.; Watanabe, Y.; Komiya, R.; Koide, N.; Han, L., *Jpn. J. Appl. Phys*. **2006**, *45*, L638–L640
13. Gao, F.Wang, Y.; Shi, D.; Zhang, J.; Wang, M.; Jing, X.; Humphry-Baker, R.; Wang, P.; et al., *J. Am. Chem. Soc*. **2008**, *130*, 10720–10728
14. Jfrank, A. J.; Kopidakis, N.; Lagemaat, J. V. D., *Coord. Chem. Rev*. **2004**, *248*, 1165–1179
15. Wang, Z. S.; Huang, C. H.; Zhang, B. W.; Hou, Y. J.; Xie, P. H.; Qian, H. J.; Ibrahim, K., *N. J. Chem*. **2000**, *24*, 567–568
16. Wang, Z. S.; Huang, C. H.; Huang, Y. Y.; Zhang, B. W.; Xie, P. H.; Hou, Y. J.; Ibrahim, K.; Qian, H. J.; et al.., *Sol. Energy Mater. Sol. Cells* **2002**, *71*, 261–271
17. Argazzi, R.; Bignozzi, C. A.; Yang, M.; Hasselmann, G. M.; Meyer, G. J., *Nano Lett*. **2002**, *2*, 625–628
18. Amadelli, R.; Argazzi, R.; Bignozzi, C. A.; Scandola, F., *J. Am. Chem. Soc*. **1990**, *112*, 7099–7103
19. Zakeeruddin, S. M.; Nazeeruddin, M. K.; Humphry-Baker, R.; Pechy, P.; Quagliotto, P.; Barolo, C.; Viscardi, G.; Gratzel, M., *Langmuir* **2002**, *18*, 952–954
20. Renouard, T.; Fallahpour, R.A.; Nazeeruddin, M. K.; Humphry-Baker, R.; Gorelsky, S. I.; Lever, A. B. P.; Grätzel, M., *Inorg. Chem*. **2002**, *41*, 367–378
21. Tsubomura, H.; Matsumura, M.; Nomura, Y.; Amamiya, T., *Nature* **1976**, *261*, 402–403
22. Sayama, K.; Sugino, M.; Sugihara, H.; Abe, Y.; Arakawa, H., *Chem. Lett*. **1998**, 753–754
23. Wang, Z. S.; Huang, Y. Y.; Huang, C. H.; Zheng, J.; Cheng, H. M.; Tian, S. J., *Synth. Met*. **2000**, *114*, 201–207
24. Sayama, K.; Hara, K.; Sugihara, H.; Arakawa, H.; Mori, N.; Satsuki, M.; Suga, S.; Tsukagoshi, S.; et al., *Chem. Commun*. **2000**, 1173–1174
25. Wang, Z. S.; Li, F. Y.; Huang, C. H., *Chem. Commun*. **2000**, 2063–2064
26. Wang, Z. S.; Li, F. Y.; Huang, C. H.; Wang, L.; Wei, M.; Jin, L. P.; Li, N. Q., *J. Phys. Chem. B* **2000**, *104*, 9676–9682
27. Hara, K.; Sayama, K.; Arakawa, H.; Ohga, Y.; Shinpo, A.; Suga, S., *Chem. Commun*. **2001**, 569–570
28. Hara, K.; Sato, T.; Katoh, R.; Furube, A.; Ohga, Y.; Shinpo, A.; Suga, S.; Sayama, K.; et al., *J. Phys. Chem. B* **2003**, *107*, 597–606
29. Hara, K.; Dan-oh, Y.; Kasada, C.; Ohga, Y.; Shinpo, A.; Suga, S.; Sayama, K.; Arakawa, H., *Langmuir* **2004**, *20*, 4205–4210
30. Hara, K.; Kurashige, M.; Ito, S.; Shinpo, A.; Suga, S.; Sayama, K.; Arakawa, H., *Chem. Commun*. **2003**, 252–253
31. Hara, K.; Sato, T.; Katoh, R.; Furube, A.; Yoshihara, T.; Murai, M.; Kurashige, M.; Ito, S.; et al., *Adv. Funct. Mater*. **2005**, *15*, 246–252
32. Kitamura, T.; Ikeda, M.; Shigaki, K.; Inoue, T.; Anderson, N. A.;

Ai, X.; Lian, T.; Yanagida, S., *Chem. Mater*. **2004**, *16*, 1806–1812

33. Xu, W.; Peng, B.; Chen, J.; Liang, M.; Cai, F., *J. Phys. Chem. C* **2008**, *112*, 874–880
34. Tian, H.; Yang, X.; Cong, J.; Chen, R.; Liu, J.; Hao, Y.; Hagfeldt, A.; Sun, L., *Chem. Commun*. **2009**, 6288–6290
35. Hara, K.; Kurashige, M.; Dan-oh, Y.; Kasada, C.; Shinpo, A.; Suga, S.; Sayama, K.; Arakawa, H., *N. J. Chem*. **2003**, *27*, 783–785
36. Hara, K.; Wang, Z. S.; Sato, T.; Furube, A.; Katoh, R.; Sugihara, H.; Dan-Oh, Y.; Kasada, C.; et al., *J. Phys. Chem. B* **2005**, *109*, 15476–15482
37. Hagberg, D. P.; Marinado, T.; Karlsson, K. M.; Nonomura, K.; Qin, P.; Boschloo, G.; Brinck, T.; Hagfeldt, A.; et al., *J. Org. Chem*. **2007**, *72*, 9550–9556
38. Liu, W. H.; Wu, I. C.; Lai, C. H.; Lai, C. H.; Chou, P. T.; Li, Y. T.; Chen, C. L.; Hsu, Y. Y.; et al., *Chem. Commun*. **2008**, 5152–5154
39. Justin Thomas, K. R.; Hsu, Y.C.; Lin, J. T.; Lee, K.M.; Ho, K.C.; Lai, C.H.; Cheng, Y.M.; Chou, P.T., *Chem. Mater*. **2008**, *20*, 1830–1840
40. Yum, J. H.; Hagberg, D. P.; Moon, S. J.; Karlsson, K. M.; Marinado, T.; Sun, L. C.; Hagfeldt, A.; Nazeeruddin, M. K.; et al., *Angew. Chem. Int. Ed*. **2009**, *48*, 1576–1580
41. Moon, S. J.; Yum, J. H.; Humphry-Baker, R.; Karlsson, K. M.; Hagberg, D. P.; Marinado, T.; Hagfeldt, A.; Sun, L. C.; et al., *J. Phys. Chem. C* **2009**, *113*, 16816–16820
42. Kim, S.; Lee, J. K.; Kang, S. O.; Ko, J.; Yum, J. H.; Fantacci, S.; De Angelis, F.; Di Censo, D.; et al., *J. Am. Chem. Soc*. **2006**, *128*, 16701–16707
43. Baik, C.; Kim, D.; Kang, M.S.; Song, K.; Kang, S. O.; Ko, J., *Tetrahedron* **2009**, *65*, 5302–5307
44. Choi, H.; Lee, J. K.; Song, K. H.; Song, K.; Kang, S. O.; Ko, J., *Tetrahedron* **2007**, *63*, 1553–1559
45. Chen, R.; Yang, X.; Tian, H.; Wang, X.; Hagfeldt, A.; Sun, L., *Chem. Mater*. **2007**, *19*, 4007–4015
46. Xu, M.; Wenger, S.; Bala, H.; Shi, D.; Li, R.; Zhou, Y.; Zakeeruddin, S. M.; Grätzel, M.; et al., *J. Phys. Chem. C* **2009**, *113*, 2966–2973
47. Wang, M.; Xu, M.; Shi, D.; Li, R.; Gao, F.; Zhang, G.; Yi, Z.; Humphry-Baker, R.; et al., *Adv. Mater*. **2008**, *20*, 4460–4463
48. Xu, M.; Li, R.; Pootrakulchote, N.; Shi, D.; Guo, J.; Yi, Z.; Zakeeruddin, S. M.; Grätzel, M.; et al., *J. Phys. Chem. C* **2008**, *112*, 19770–19776
49. Zhang, G.; Bai, Y.; Li, R.; Shi, D.; Wenger, S.; Zakeeruddin, S. M.; Grätzel, M.; Wang, P., *Energy Environ. Sci*. **2009**, *2*, 92
50. Chen, R.; Yang, X.; Tian, H.; Wang, X.; Hagfeldt, A.; Sun, L., *Chem. Mater*. **2007**, *19*, 4007–4015
51. Qin, H.; Wenger, S.; Xu, M.; Gao, F.; Jing, X.; Wang, P.; Zakeeruddin, S. M.; Grätzel, M., *J. Am. Chem. Soc*. **2008**, *130*, 9202–9203
52. Zhou, G.; Pschirer, N.; Schöneboom, J.; Eickemeyer, F.; Baumgarten, M.; Müllen, K., *Chem. Mater*. **2008**, *20*, 1808–1815
53. Jiang, K. J.; Manseki, K.; Yu, Y. H.; Masaki, N.; Xia, J. B.; Yang, L. M.; Song, Y. L.; Yanagida, S., *N. J. Chem*. **2009**, *33*, 1973–1977
54. Li, G.; Jiang, K. J.; Bao, P.; Li, Y. F.; Li, S. L.; Yang, L. M., *N. J. Chem*. **2009**, *33*, 868
55. Wang, Z. S.; Cui, Y.; Dan-Oh, Y.; Kasada, C.; Shinpo, A.; Hara, K., *J. Phys. Chem. C* **2007**, *111*, 7224–7230
56. Wang, Z. S.; Cui, Y.; Hara, K.; Dan-oh, Y.; Kasada, C.; Shinpo, A., *Adv. Mater*. **2007**, *19*, 1138–1141
57. Wang, Z. S.; Cui, Y.; Dan-oh, Y.; Kasada, C.; Shinpo, A.; Hara, K., *J. Phys. Chem. C* **2008**, *112*, 17011–17017
58. Zhang, G.; Bala, H.; Cheng, Y.; Shi, D.; Lv, X.; Yu, Q.; Wang, P., *Chem. Commun*. **2009**, 2198–2200
59. Wang, Z. S.; Hara, K.; Dan-oh, Y.; Kasada, C.; Shinpo, A.; Suga, S.; Arakawa, H.; Sugihara, H., *J. Phys. Chem. B* **2005**, *109*, 3907–3914
60. Liu, B.; Zhu, W.; Zhang, Q.; Wu, W.; Xu, M.; Ning, Z.; Xie, Y.; Tian, H., *Chem. Commun*. **2009**, 1766–1768
61. Ning, Z.; Zhang, Q.; Wu, W.; Pei, H.; Liu, B.; Tian, H., *J. Org. Chem*. **2008**, *73*, 3791–3797
62. Koumura, N.; Wang, Z. S.; Mori, S.; Miyashita, M.; Suzuki, E.; Hara, K., *J. Am. Chem. Soc*. **2006**, *128*, 14256–14257
63. Wang, Z. S.; Koumura, N.; Cui, Y.; Takahashi, M.; Sekiguchi, H.; Mori, A.; Kubo, T.; Furube, A.; et al., *Chem. Mater*. **2008**, *20*, 3993–4003
64. Wang, Z. S.; Koumura, N.; Cui, Y.; Miyashita, M.; Mori, S.; Hara, K., *Chem. Mater*. **2009**, *21*, 2810–2816
65. Qu, S.; Wu, W.; Hua, J.; Kong, C.; Long, Y.; Tian, H., *J. Phys. Chem. C* **2010**, *114*, 1343–1349
66. Wu, W.; Yang, J.; Hua, J.; Tang, J.; Zhang, L.; Long, Y.; Tian, H., *J. Mater. Chem*. **2010**, *20*, 1772
67. Tang, J.; Wu, W.; Hua, J.; Li, J.; Li, X.; Tian, H., *Energy Environ. Sci*. **2009**, *2*, 982
68. Pei, J.; Peng, S.; Shi, J.; Liang, Y.; Tao, Z.; Liang, J.; Chen, J., *J. Power Sources* **2009**, *187*, 620–626
69. Xu, W.; Pei, J.; Shi, J.; Peng, S.; Chen, J., *J. Power Sources* **2008**, *183*, 792–798
70. Shi, J.; Peng, S.; Pei, J.; Liang, Y.; Cheng, F.; Chen, J., *ACS Appl. Mater. Interf*. **2009**, *1*, 944–950
71. Liang, M.; Xu, W.; Cai, F.; Chen, P.; Peng, B.; Chen, J.; Li, Z., *J. Phys. Chem. C* **2007**, *111*, 4465–4472
72. Ning, Z.; Tian, H., *Chem. Commun*. **2009**, 5483–5495
73. Zhang, Q.; Ning, Z.; Pei, H.; Wu, W., *Front. Chem. China* **2009**, *4*, 269–277